Composite Structures 295 (2022) 115755

Contents lists available at ScienceDirect

Composite Structures

journal homepage: www.elsevier.com/locate/compstruct

Enhancement of vibration attenuation and shock absorption in composite sandwich structures with porous foams and surface patterns

Hoo Min Lee, Do Hyeong Kim, Dong-Yoon Kim, Min Seong Kim, Junhong Park, Gil Ho Yoon *

Department of Mechanical Engineering, College of Engineering, Hanyang University, Seoul, 04763, Republic of Korea

ARTICLE INFO

Keywords:
Composite sandwich structure
Porous foam
Surface pattern
Vibration attenuation
Shock absorption
Mass reduction

ABSTRACT

In the present study, composite sandwich structures were investigated to evaluate the effects of porous foams and surface patterns on structural stability and mass reduction of the composite sandwich structures. The composite structures used in the experiments consisted of three layers; the top and bottom polycarbonate (PC) layers and the core porous foam layers. Copper, nickel, and polypropylene (PP) foams were considered in the modeling of composite structures. Laser cutting technology was applied to the top PC layers of the composite structures to realize the surface patterns. Impact hammer and mass drop tests were performed on the composite structures to investigate their vibration attenuation and shock absorption performances. Numerous combinations of composite structures were considered by varying the foam materials and layer thicknesses to determine the best configuration. Finite element method (FEM)-based simulations were conducted to verify the experimental results. The results of this study support the implementation of porous foams and surface patterns for the increase in vibration attenuation and shock absorption performance, while achieving mass reduction for various applications in the engineering field.

1. Introduction

The present study evaluates the effects of porous foams and surface patterns on structural stability and mass reduction of composite structures. The composite structures considered in this study were composed of three layers. The top and bottom layers consisted of polycarbonate (PC) plates, and the core layers consisted of porous foams. Copper, nickel, and polypropylene (PP) foams were considered as the core materials. Laser cutting technology was applied to the top PC layers to realize the surface patterns. Impact hammer tests and mass drop tests were performed on the composite structures to analyze their vibration attenuation and shock absorption performance. Various combinations of composite structures were considered by changing the core foam materials, modifying the core thicknesses, and considering the surface patterns. Analyses and comparisons were performed to realize the best configuration with maximized vibration attenuation and shock absorption performance, while achieving mass reduction. Simulations using finite element method (FEM) were conducted to verify the experimental results.

Structural instability due to vibrational motion, external impact, and excessive weight, is an important engineering subject. Composite structures have received attention for their potential to resolve the instability arising from these factors. Relevant research has been performed on impact-induced vibrations in honeycomb sandwich panels [1] and the post-impact vibration response of protective sandwich plates [2], resulting in vibration analyses for composite structures. Moreover, studies have been conducted to analyze impact resistance of composite structures. Studies have also been conducted to investigate the impact response of flat steel-concrete-corrugated steel sandwich panels [3], dynamic impact response of tubular sandwich structures [4], low-velocity impact response of sandwich panels [5], and static and impact behavior of polymer composite beams [6]. Based on the analyses of composite structures, various methods have been introduced to increase the vibration attenuation and shock absorption performance. Methods using periodic stitches [7], internal explosions using composite materials [8], anti-resonance frequencies [9], negative stiffness nonlinear oscillators [10], elastically restrained sandwich window pane [11], and ultra-thin sandwich pane [12], have been proposed to achieve vibration attenuation of composite structures. New origami-inspired honeycomb sandwich plates [13], sandwich panels with aramid honeycomb [14], panels with improved composite design [15], and structures with textile-reinforced fold-cores [16], have been proposed to increase the shock absorption performance and impact strength of the composite structures. The minimization of mass and stress concentrations [17] and absorption of electromagnetic waves [18] are also possible by utilizing composite structures.

* Corresponding author.
E-mail address: ghy@hanyang.ac.kr (G.H. Yoon).

https://doi.org/10.1016/j.compstruct.2022.115755
Received 24 December 2021; Received in revised form 23 March 2022; Accepted 8 May 2022
Available online 20 May 2022

The proposed methods generally focus on modification of composite structural designs. In addition to changing structural designs, studies have been conducted on the effect of materials for achieving structural stability of composite structures. Methods using metal foams [19–23], polycarbonate foams [24,25], and thermoplastic foams [26,27], have been proposed to modify the impact strength, thermo-mechanical properties, and wave propagation characteristics of composite structures. Studies have also been conducted on the effect of structural designs, where methods using dual panels [28], optically transparent and flexible absorbers [29], and sandwich meta-absorbers [30], have been proposed for the modification of stress waves, transmittance of certain frequency waves, and dissipation of energy. Research has also been conducted on the effects of Y-shaped cores on mechanical properties and energy absorption capacities [31], and studies have shown that the simultaneous application of foam materials and modification of structural design are capable of enhancing bending stiffness and failure loads of composite sandwich structures [32]. In [33,34], experimental and numerical analyses of low velocity impact test were conducted to evaluate dynamic behaviors and determine optimal designs based on energy absorption criterion. Hence, the latest studies considering composite sandwich structures focus on enhancement of various mechanical properties. Our study aims to step further, by investigating sandwich structural design capable of achieving mass reduction, increasing vibration attenuation, and enhancing shock absorption simultaneously by applying foam materials as well as modifying the structural design using surface patterns. The proposed method attempts to determine the composite sandwich design of best configuration with enhanced structural stability and resistance to vibrational motions and external impacts.

The present research aims to realize the best configuration of composite sandwich structures using porous foams and surface patterns, as shown in Fig. 1, to maximize vibration attenuation and shock absorption, while achieving mass reduction. The composite structures consist of PC plates and porous foams with constant pore per inch (PPI) values. The foam materials considered were copper, nickel, and PP foams. The composite structures were designed to have top and bottom PC layers with core porous foam layers in the middle. The three layers of the composite structures are merged using strong adhesion at the edges and compressed during the manufacturing process to remove residual air between the layers of the structures. Surface patterns were formed on the top layers of the composite structures using laser cutting technology, with depth values of half the thicknesses of the PC layers. After modeling the composite structures, experiments were performed to evaluate their vibration attenuation and shock absorption performance. Impact hammer tests were performed by triggering transverse vibrations using an impact hammer to obtain frequency response functions for vibration response analysis. Mass drop tests were performed by dropping impactors to obtain the impact force for the shock absorption analysis. Various combinations of composite structures were considered in the experimental study to compare the mass reduction rates, vibration attenuation performance, and shock absorption performance. Comparisons are made between structures with and without the surface patterns, structures with different core thicknesses, and structures with different core materials. Analyses and comparisons were performed to determine the best configuration of the composite sandwich structure for maximizing the vibration attenuation and shock absorption performance. FEM-based simulations using COMSOL and ANSYS workbench were performed to verify the experimental results of the proposed sandwich structures. Vibration analyses and reaction force analyses were conducted to validate the vibration attenuation and shock absorption performance of the proposed composite sandwich structure.

The remainder of this paper is organized as follows. Section 2 provides some background to the manufacturing of composite structures and the experimental method used to evaluate vibration attenuation and shock absorption performances. Section 3 presents the mathematical theory of data processing performed in this study. Section 4 presents the analyses of experimental and simulation results to determine the best configuration of the composite sandwich structure. Conclusions and future topics are discussed in Section 5.

2. Experimental method

Several experiments were carried out to investigate the effects of the surface patterns, core thickness, and the core material of the composite structure on the vibration attenuation and shock absorption functions. The effects of the surface patterns were evaluated by comparing the 5 mm PC plates with and without the surface patterns. The effect of the thickness of the core porous material was evaluated by comparing composite structures with 2–3 mm core thickness. With a constraint of 5 mm for the total thickness, the thickness of the top PC layer was also varied. In addition, the effects of the core materials were evaluated by comparing structures with core copper foam layers, core nickel foam layers, and core PP foam layers.

2.1. Manufacturing of composite structure

The composite sandwich structures of interest consisted of the top and bottom PC layers and core porous foam layers. In the present study, the length and width of the layers were 500 mm × 500 mm. The three foams, that is, copper, nickel, and PP foams, were considered and investigated for the core porous foam materials. All the core foams had constant porosity and pore density, with values of 0.98 and 60 PPI (pores per inch), respectively. The composite structures were manufactured by merging the layers using adhesive wax and oriented PP adhesive at the edges. The adhesive was only daubed at the edges and not on the entire interface between the skins and core to prevent the creation of extra adhesive layers or permeation of wax into the pores of the foam material. During this manufacturing process, the layers were compressed using an F2C-T31 heat press combo machine, as shown in Fig. 2(a), to remove residual air between the layers. After the merging process, the laser cutting (Innosta IS-1290 laser cutter shown in Fig. 2(b)) was used to carve the surface patterns on the top PC layers. The cutting speed was set at a constant value of 8.5 mm/s. The surface patterns were realized to have lane-type designs with a depth of half the thicknesses of the PC layers. The patterns, with a depth of 0.5 mm, were carved using 14.69 W of laser power on 1 mm thick PC layers. The patterns, with a depth of 1 mm, were carved using 19.50 W of laser power onto the PC layers of 2 mm thickness. Five lane type patterns were carved on each PC layer, where the patterns were 50 mm apart from each other, and the pattern in the center was positioned along the middle of the plate. Fig. 2(c) shows an illustration of the modeled composite structures. In addition, the surface patterns were also carved on the PC plates with a thickness of 5 mm, for comparison with PC plates without the surface patterns. The patterns were carved to a depth of 2.5 mm, and this was realized using 26.00 W of laser power using the Innosta IS-1290 laser cutter.

2.2. Comparison of structural mass

Comparison of structural masses of manufactured structures were made to evaluate the effects of foam materials and their thicknesses on mass reduction. Surface patterns were not considered, as they showed a negligible effect on mass reduction. The masses of six composite specimens were compared with those of the reference PC specimen. Note that two different composite designs, with core thicknesses of 2 mm and 3 mm, respectively, and three different core materials were considered, which comprised six combinations of composite specimens. All seven specimens had a total thickness of 5 mm. The masses of the specimens are listed in Table 1. From the table, it can be seen that the composite specimen with a nickel foam core of 3 mm thickness shows

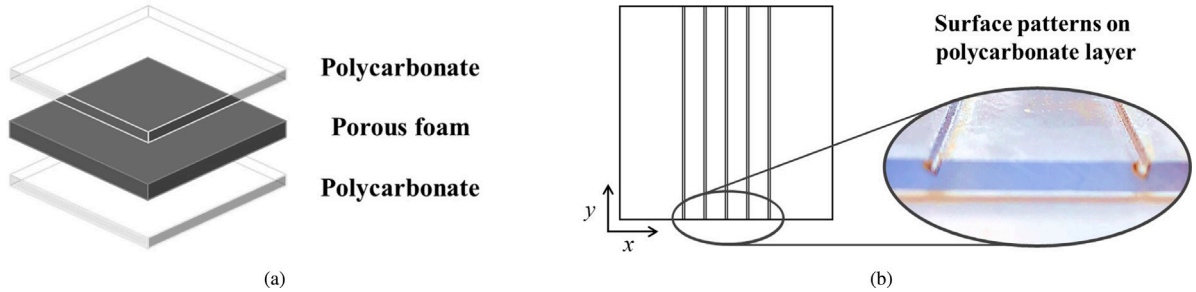

Fig. 1. Composite structure mechanism: (a) Three-layer composite sandwich structure and (b) surface patterns realized on polycarbonate layer to attenuate vibration in x-direction.

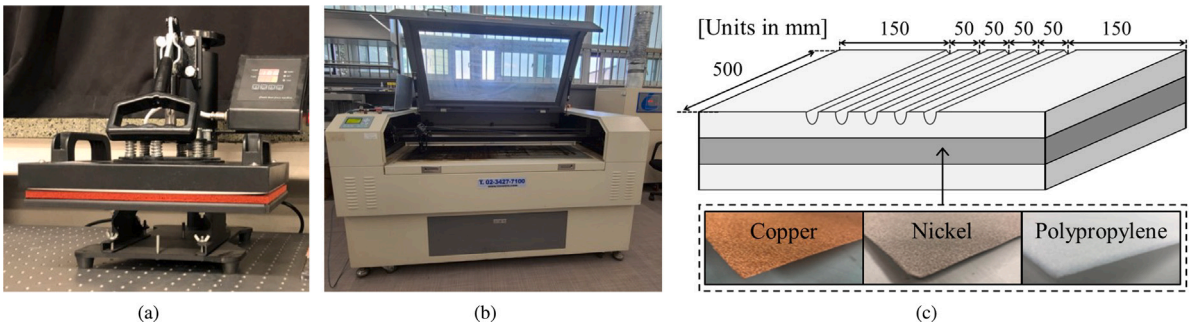

Fig. 2. (a) F2C-T31 heat press combo machine utilized for merging of the layers, (b) Innosta IS-1290 laser cutter used for realization of surface pattern design, and (c) illustration of the modeled composite structure and its dimensions.

Table 1
Mass comparison of specimens.

Specimen	Foam material	Structure thickness (mm)				Structure mass (kg)		Relative mass to reference specimen (%)
		Top layer	Porous foam	Bottom layer	Total	Porous foam	Total	
1 (Reference)	–	5	-	-	5	-	1.480	100
2	Copper	1	3	1	5	0.633	1.253	84
3	Copper	2	2	1	5	0.223	1.144	77
4	Nickel	1	3	1	5	0.111	0.713	48
5	Nickel	2	2	1	5	0.125	1.046	70
6	Polypropylene	1	3	1	5	0.326	0.928	62
7	Polypropylene	2	2	1	5	0.226	1.147	77

the greatest mass reduction, with mass of 0.713 kg, and relative mass of 48% compared to the reference PC specimen. On the other hand, the composite specimen with a copper foam core of 2 mm thickness showed the least mass reduction, with mass of 1.253 kg, and relative mass of 84% compared to the reference PC specimen. The results show that the composite sandwich structures with core foam layers generally excel with regard to the mass reduction of the structures, with nickel porous foam being the most effective material for this purpose.

2.3. Impact hammer test considering transverse vibration

An impact hammer test considering transverse vibration was conducted to evaluate the vibration attenuation performance of the structures, as shown in Fig. 3. The specific parameters of the specimens utilized for the experiment are shown in Table 2. To obtain accurate and constant experimental results, each configuration was tested five times, and the mean values were evaluated. Two fixed frames were connected with rubber bands, and the structure being tested was placed on the rubber bands to achieve free-free boundary condition. Note that hanging structures better satisfy the free-free boundary condition. As shown in Appendix A, the hanging method showed better agreement with numerical simulations. However, due to difficulties of applying constant forces to the hanging structure, the experimental method of placing structures on rubber bands was employed for the impact hammer test. Low-frequency transverse vibration signals were triggered using an ICP-type impact hammer (PCB Piezotronics model 086C03). It was ensured that the forces triggered by the impact hammer had constant values, by only accepting input forces within the 14–16 N range. The vibration responses were measured using a uniaxial accelerometer (PCB Piezotronics model 352C33), which was installed on the structure using adhesive wax. The impact hammer triggered point and accelerometer installation points are shown in Fig. 3. Note that the surface patterns are between the two points to ensure that the vibrational motions were affected by the patterns. The measured data were generated and processed using a data acquisition device with a vibration input module (NI cDAQ-9171, NI 9234), and analyzed using Fourier transforms to obtain time-dependent signals in the frequency domains. The vibration attenuating characteristics of the structures were evaluated by comparing and analyzing the vibration responses.

2.4. Mass drop test with round-ended impactor

The mass drop test was conducted to evaluate the shock absorption performance of the structures, as shown in Fig. 4. The specific parameters of the specimens utilized for the experiment are shown in Table 2. To obtain accurate and constant experimental results, five specimens for each configuration were tested, and the mean values were evaluated. A drop impactor tester and data acquisition device (NI

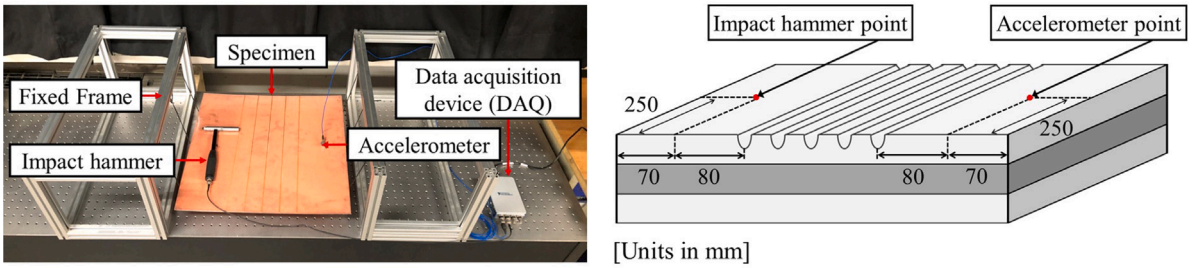

Fig. 3. Impact hammer test equipment setup.

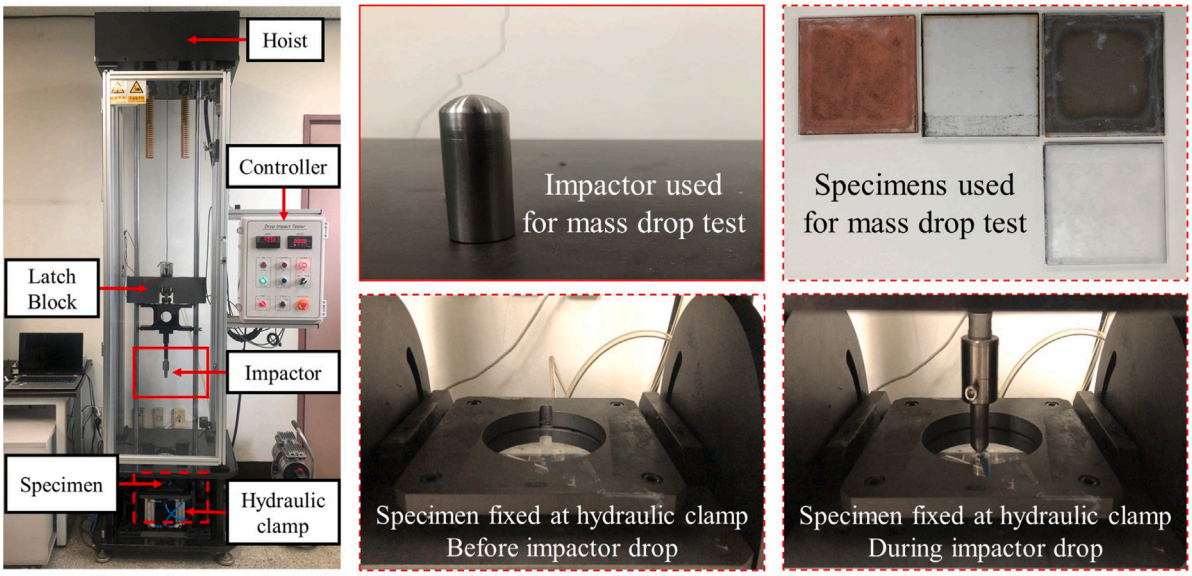

Fig. 4. Mass drop test equipment setup.

Table 2
Parameters of specimens utilized for impact hammer and mass drop experiments.

Material	Specimen size for each experiment		Young's modulus (MPa)	Poisson's ratio	Density (kg/m^3)
	Impact hammer	Mass drop			
Polycarbonate	500 mm × 500 mm	120mm × 120 mm	2500	0.36	1200
Copper	500 mm × 500 mm	120 mm × 120 mm	740	0.34	1000
Nickel	500 mm × 500 mm	120 mm × 120 mm	200	0.30	450
Polypropylene	500 mm × 500 mm	120 mm × 120 mm	1000	0.33	910

USB 6351) were used for the mass drop experiment. The structure was fixed using a round hydraulic clamp. The hoist and controller were used to control and move the latch block to the desired height. The impactors were connected to this latch block in a detachable manner. Among the various impactors with different tip geometries, the impactor used in the experiment had a round end, with a diameter of 1.6 cm and a mass of 2 kg. To evaluate the shock absorption performance, the round-ended impactor was dropped from a constant height of 500 mm, and a sensor attached to the latch block was used to measure the magnitudes of the impact forces. The measured impact forces were used to evaluate the shock absorption performance using the ISG software connected to the tester. Note that structures with greater shock absorption characteristics result in lower impact force values. The shock absorption properties of the structures were evaluated by comparing and analyzing the impact forces.

3. Data processing

To compare the dynamic and collision characteristics of the composite plates depending on their manufacturing approaches, the following analyses were carried out—frequency response and impact energy analyses using the data collected from the impact hammer and mass drop tests. The data processing process allowed the evaluation of material choice of the porous layer and presence of surface patterns.

3.1. Frequency response function using transverse vibration

The vibration data of the composite plates from the impact hammer test were measured, and the frequency response functions (FRFs) of the measured vibration data were calculated to compare and characterize the vibration attenuation performance of the composite plates. The natural frequencies of the plates were compared in the process. In addition, the dynamic properties of the plates, that is, stiffness, mass, and damping, were analyzed and compared. In our tests, the single input and single output were measured for the frequency response functions.

With relatively simple procedures, the dynamic properties of the system such as stiffness, mass, and damping, were obtained. The equation of motion for a single degree-of-freedom system was transformed into the frequency domain through the Laplace transform method and

the frequency response is presented by the correlation between the input and output of a dynamic system. The frequency response used in the mechanical system is formulated using the input and output signals of the dynamic system as follows:

$$H(s) = \frac{X(s)}{F(s)} = \frac{1}{ms^2 + cs + k} \tag{1}$$

where the frequency response, input signal, and output signal of the dynamic system are expressed as $H(s)$, $F(s)$, and $X(s)$, respectively. The frequencies with complex value, mass, viscous damping, and stiffness are denoted by s, m, c, and k, respectively. When considering the natural frequency and damping ratio, the frequency response used in the mechanical system is formulated as follows:

$$H(s) = \frac{\frac{k}{m}}{s^2 + \frac{c}{m}s + \frac{k}{m}} \cdot \frac{1}{k} = \frac{\omega_n^2}{s^2 + 2\zeta\omega_n s + \omega_n^2} \tag{2}$$

where ω_n and ζ are the natural frequency and damping ratio, respectively. During the transverse vibration experiment, the frequency response was calculated by measuring the impact force and acceleration response of the impact hammer. The frequency response function (FRF) between the force sensor of the hammer and the acceleration sensor attached to the vibrating system of interest is as follows:

$$\text{FRF} = \frac{P_{xy}(s)}{P_{xx}(s)} \tag{3}$$

where the cross-spectrum of the input and output signals is denoted by $P_{xy}(s)$, and the auto-spectrum of the input signal is denoted by $P_{xx}(s)$. Overall, the FRF can be used to evaluate the vibration responses of materials at given impacts, to analyze their vibration attenuation performance.

3.2. Collision analysis using impact energy

The shock absorption can be evaluated by dropping an impactor on the specimen which is accelerated by gravity, that is, using the mass drop experiment shown in Fig. 5. A mathematical formulation considering the mass drop can be found in [35]. In the mass drop experiment, an impactor is dropped, and the shock absorption characteristics according to the composition or material selection of the composite are analyzed using the force applied to the structure by the impactor. For a simple one-dimensional system, the governing equation of the impactor can be formulated as follows:

$$m_i g - F_i = m_i \frac{dv}{dt}, \quad \frac{dv}{dt} = g - \frac{F_i}{m_i} \tag{4}$$

where m_i and F_i are the total mass and the average external force of the impactor, respectively, and the subscript i indicates that the corresponding quantities are those of the impactor. The gravity, velocity, and time are denoted by g, v, and t, respectively. Integrating Eq. (4) gives the velocity at any time.

$$v = v_0 + gt - \frac{1}{m_i}\int_0^t F_i dt \tag{5}$$

$$x = v_0 t + \frac{gt^2}{2} - \frac{1}{m_i}\int_0^t \left(\int_0^t F_i dt\right) dt \tag{6}$$

The displacement presented by integration is denoted by x in Eqs. (5) and (6). During the mass drop experiment, the initial velocity, denoted as v_0, indicates the velocity at the initial contact of the impactor with the specimen. The impact energy, U, during collision can be formulated as follows:

$$U = \int F_i dx \tag{7}$$

$$U = v_0 \int_0^t F_i dt + g\int_0^t tF_i dt - \frac{1}{2m_i}\left(\int_0^t F_i dt\right)^2 \tag{8}$$

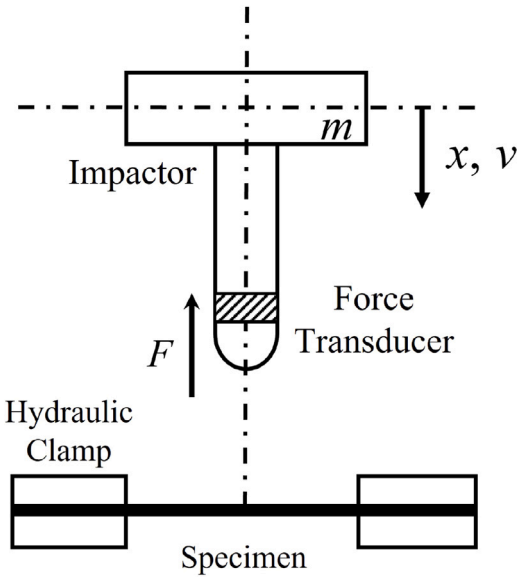

Fig. 5. The instrumented mass drop test method.

where U denotes the impact energy. The impact energy can be used to evaluate the validity of the mass drop experiments when comparing the shock absorption performances of materials. When structures are applied with equal impact energies at given impacts through impactors dropped onto them, but result in different force values due to increased collision time and greater specimen deformation, it can be evaluated that the structure resulting in lower force has greater shock absorption performance.

4. Results and discussions

The experimental and simulation results for vibration attenuation and shock absorption performance are presented in this section. The effects of surface patterns, core thickness values, and core materials are discussed to determine the best configuration of the suggested composite sandwich structures, to achieve structural stability.

4.1. Vibration attenuation performances

Through the impact hammer test, the vibration responses of the specimens were analyzed to evaluate their vibration attenuation performance. The effects of the surface patterns were evaluated by comparing the PC specimens with and without the pattern designs. Both types of specimens had thickness values of 5 mm. The vibration responses of both specimens are shown in Fig. 6(a). Both specimens have natural frequencies of 33, 43, and 82 Hz. It can be seen that the PC specimens with the surface patterns have smaller peak values at each natural frequency value. This indicates that the presence of surface patterns contributes to the increase in vibration attenuation performance, specifically at the natural frequencies of the structures. Additionally, shifting of natural frequencies could be observed when surface patterns were realized. This phenomenon could be better observed when pattern parameters were varied. The effects of changing surface pattern parameters are presented in Appendix B.

The effects of the various core thicknesses were evaluated by comparing composite specimens of the same core materials with different core layer thicknesses. Note that all the composite specimens included surface patterns on the top PC layers. The vibration responses of the composite specimens are shown in Figs. 6(b), (c), and (d). Generally, all composite specimens show a significant increase in vibration attenuation performance compared to the PC specimen. However, the

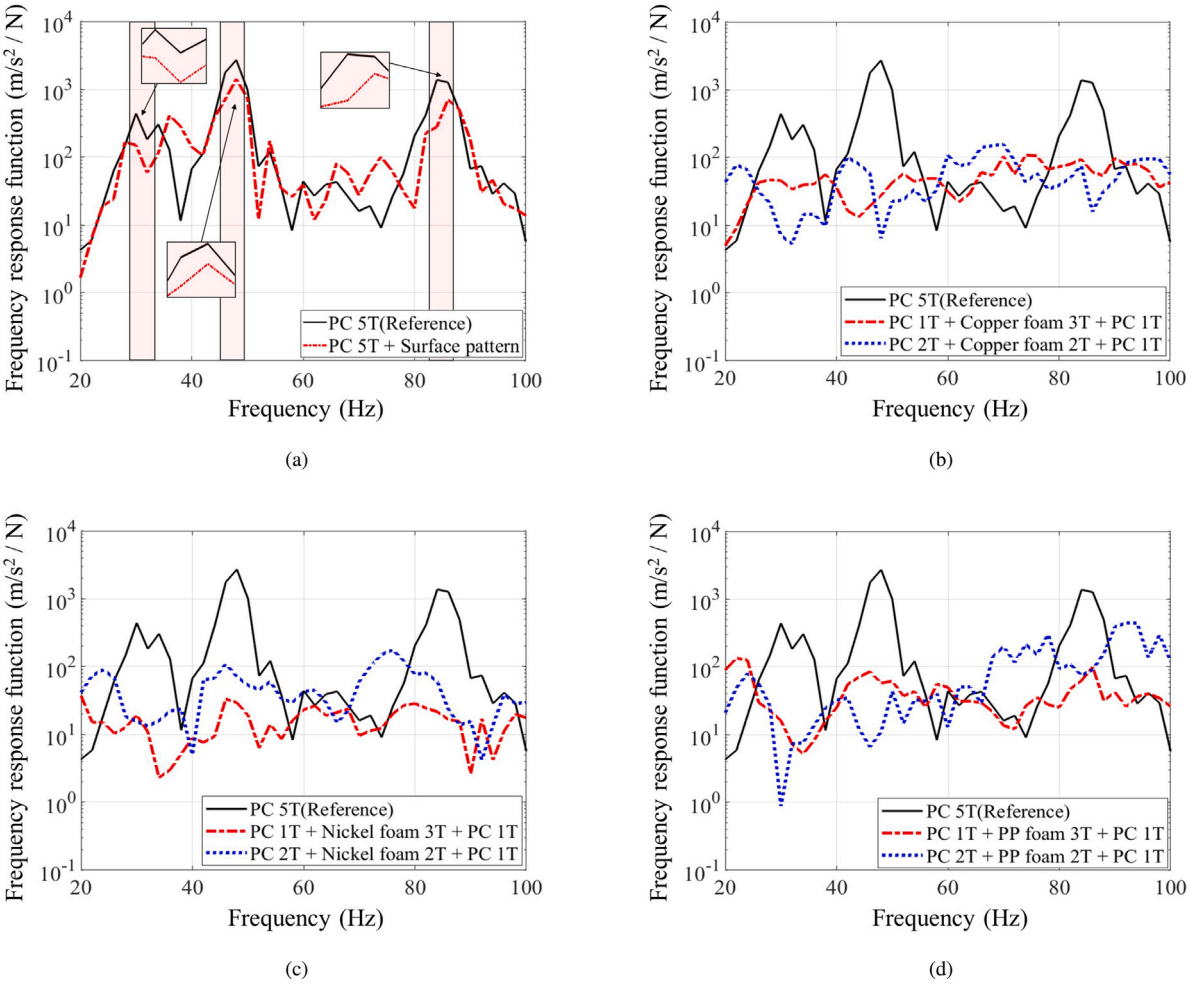

Fig. 6. Transverse vibration experiment results: (a) PC specimens with and without surface pattern designs, (b) PC and composite specimens with core copper foam layers, (c) PC specimen and composite specimens with core nickel foam layers, and (d) PC specimen and composite specimens with core PP foam layers.

effects of the core thickness vary for different core materials. In the case of copper foams, the structures with the core foam layers of 2 mm thickness resulted in the smallest peak values at natural frequencies. On the other hand, for the nickel foams, the structures with the core foam layers of 3 mm thickness showed the greatest vibration attenuation performance. For the PP foams, the structures with the core foam layers of 2 mm thickness resulted in greater vibration reduction in the 20–60 Hz range, while the structures with the core foam layers of 3 mm thickness resulted in greater vibration reduction from 60 Hz onward. Note that differences in core thicknesses do not lead to observable differences in the vibration attenuation performance, and also do not yield consistent results.

The effects of core materials were evaluated by comparing composite specimens with identical core thicknesses but different core materials. Note that all the composite specimens included surface patterns on the top PC layers. The vibration responses are shown in Fig. 7. Generally, all composite specimens showed a significant increase in vibration attenuation performance compared to the PC specimen. However, the effects of the core materials varied for different core thicknesses. For structures with core thicknesses of 2 mm, the structures with PP foams exhibited the smallest peak values at natural frequencies. For structures with core thicknesses of 3 mm, the structures with nickel foams showed the greatest vibration attenuation performance in general. The vibration attenuation performances of different configurations are summarized in Table 3, by comparing the FRF values at the eigenfrequencies. Combining and summarizing the results, the structures with PP foam of 2 mm had the most vibration reduction in the 20–60 Hz range, while the structures with nickel foam of 3 mm exhibited the greatest vibration reduction from 60 Hz onward.

4.2. Shock absorption performances

Through the mass drop test, the impact forces of the specimens were measured to evaluate their shock absorption performance. Surface patterns were not considered, as they had a negligible effect on the increase in shock absorption performance. A total of six composite specimens were considered to compare their shock absorption performance with that of the PC specimen. All seven specimens had a total thickness of 5 mm. Fig. 8 shows the impact forces of the specimens. It can be seen that the composite specimen with the nickel foam core of 3 mm thickness resulted in the greatest impact force reduction, with an impact force value of 1.638 kN. The composite specimen with the copper foam core of 2 mm thickness resulted in the least impact force reduction, with an impact force value of 2.324 kN. The results show that the composite sandwich structures with core foam layers generally show increased shock absorption performance with reduced impact force values upon contact with impactors dropped from a constant height of 500 mm.

The results show that the specimens with a core nickel foam of 3 mm thickness and surface patterns are the best configuration for the suggested sandwich structure. In terms of mass reduction, the specimen with 3 mm nickel foam showed the greatest mass reduction, with a mass of 48% compared to the PC specimen. In terms of vibration

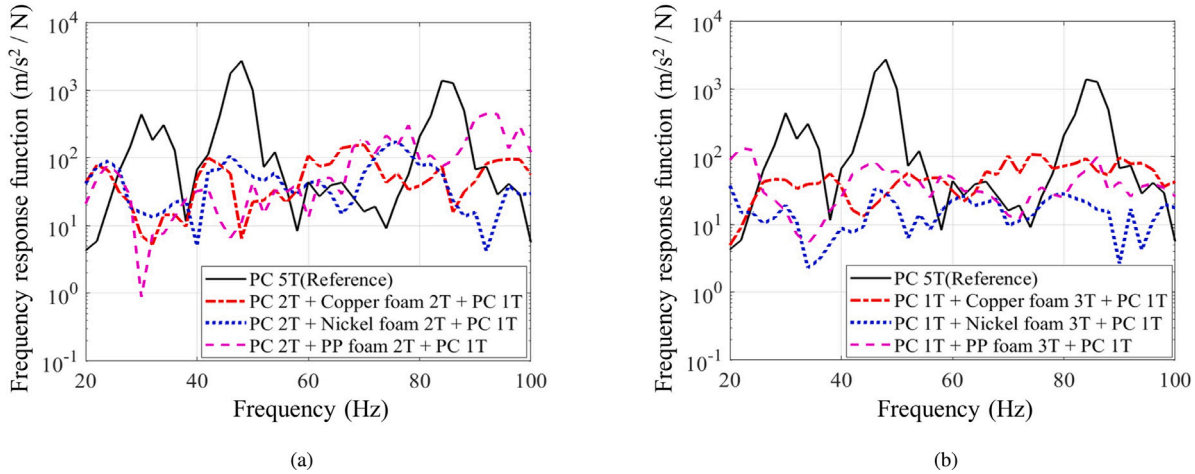

Fig. 7. Transverse vibration experiment results: (a) Composite specimens with core thickness values of 2 mm and (b) composite specimens with core thickness values of 3 mm.

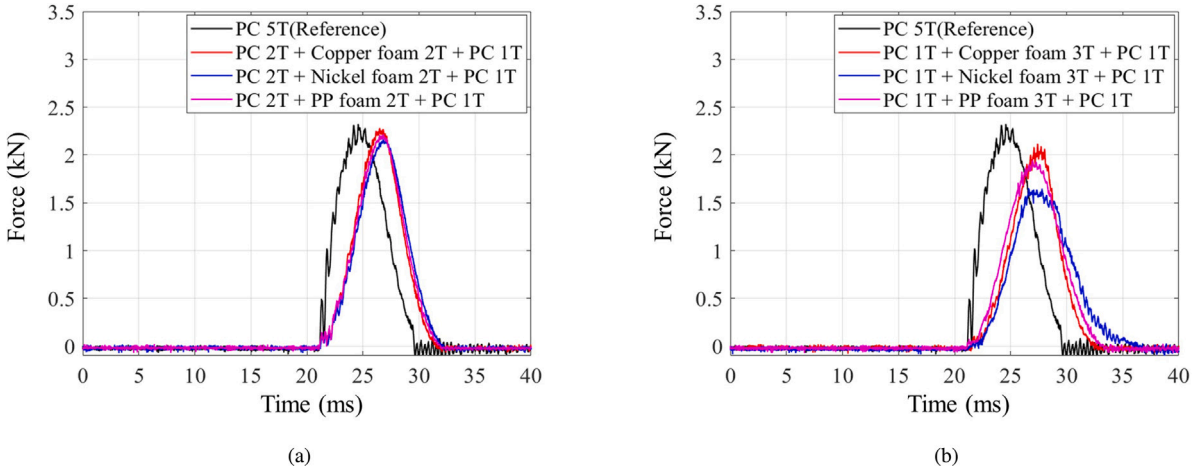

Fig. 8. Shock absorption experiment results: (a) Composite specimens with core thickness values of 2 mm and (b) composite specimens with core thickness values of 3 mm.

Table 3
FRF amplitude values of specimens at eigen-frequency values.

Mode	Frequency	Frequency response function amplitude ((m/s²)/N)							
		No surface patterns	With surface patterns						
		No foam	No foam	Copper foam 3T	Copper foam 2T	Nickel foam 3T	Nickel foam 2T	PP foam 3T	PP foam 2T
1	33 Hz	440.952	150.088	45.561	7.070	19.318	15.486	16.007	0.880
2	43 Hz	2707.14	1419.16	27.429	6.432	29.410	70.900	57.549	11.063
3	82 Hz	1379.27	279.828	93.905	75.674	21.576	60.056	62.850	74.638

attenuation, the presence of patterns resulted in smaller peak values at natural frequencies. For comparison between materials, the specimens with 3 mm nickel foam generally showed the greatest vibration reduction. In terms of shock absorption, the specimen with 3 mm nickel foam resulted in the smallest impact force value of 1.638 kN, and consequently, the greatest shock absorption performance among all the tested specimens. In summary, a composite sandwich structure with a core nickel foam layer of 3 mm and surface patterns was realized as the best configuration for maximized mass reduction, vibration attenuation, and shock absorption.

4.3. Finite element method based simulations

FEM-based simulations were conducted to verify the experimental results. COMSOL and ANSYS workbench were used to perform the vibration analysis and impact force analysis, to validate the vibration attenuation and shock absorption. The default configuration (PC specimen) and the best configuration (specimen with 3 mm nickel foam) were considered for comparison using finite element-based simulations. For the vibration analysis, the structural mechanics module of the COMSOL software was utilized to compute the response of the structure subjected to excitation using the FRF. The finite-element simulation process of the vibration analysis allows the identification of eigen-frequencies and the plotting of FRF against frequency values. PC plates and a sandwich structure with a core nickel foam of 3 mm were modeled and simulated. The modeled structures had their parameters equal to those of the real structures. The Young's modulus, Poisson's ratio, and density of polycarbonate were set as 2.5 GPa, 0.36, and 1200 kg/m^3, respectively. The Young's modulus, Poisson's ratio, and density of the nickel foam were set as 207 MPa, 0.30, and 450 kg/m^3, respectively. In addition, Rayleigh damping was considered by setting the damping coefficient as 1×10^{-6}. Tetrahedral elements with mesh size varying between 0.005 m and 0.04 m were used in all model

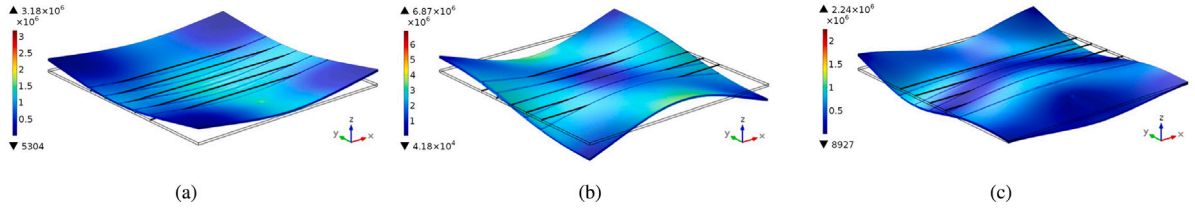

Fig. 9. Illustration of finite element vibration analysis using COMSOL: PC plate with surface patterns. (a) First mode shape at 33 Hz, (b) second mode shape at 48 Hz, and (c) third mode shape at 85 Hz.

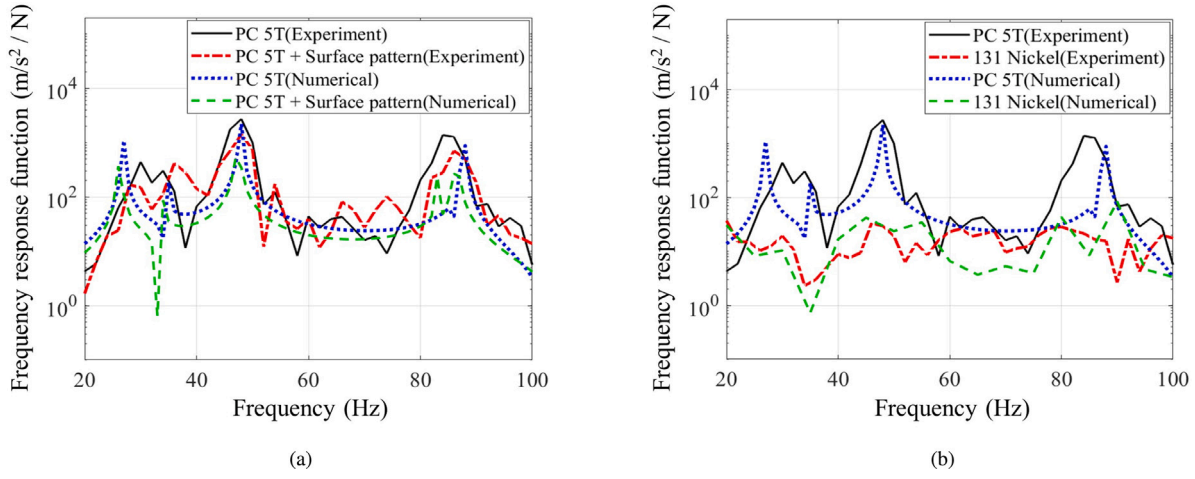

Fig. 10. Comparison between vibration experiment and vibration simulation. (a) PC specimens with and without surface pattern designs and (b) PC specimens and composite specimens with nickel core thickness values of 3 mm.

components. The composite structures were bonded completely, and the surface patterns were realized to have a constant width of 1 mm and a depth of half the value of the PC layer thickness. The excitation point and the measurement point were set at identical locations to those of the impact hammer and accelerometer points, as shown in Fig. 3. The boundary conditions were set as free-free boundary conditions, and the force applied to the excitation point was set to 15 N. Fig. 9 illustrates the finite element vibration analysis process using the COMSOL software. Fig. 10 shows the results of the vibration simulations.

Fig. 10(a) shows the experimental and simulation results of PC plates with and without the surface patterns. From the FRF graph, it can be observed that both the experiment and simulation result in similar natural frequency values. Note that perfect agreement of natural frequency values are not realized as free-free boundary conditions were not fully fulfilled during the impact hammer tests. Moreover, the results do show some differences in absolute peak values. Still, the simulation results show similar tendency to the experimental results, where the presence of the surface patterns reduces the peak values at each natural frequency value. As a result, the FEM simulation of vibration analysis validates the vibration attenuation resulting from the presence of surface patterns. Fig. 10(b) shows the experimental and simulation results of composite sandwich structure with 3 mm thickness core nickel foam, and PC plate without surface patterns for reference. Note that the modeled composite structure has surface patterns on the top PC layer. From the FRF graph, the simulation results show similar tendency to the experimental results. For both experimental and simulation results, it can be observed that the composite structure's response values are similar to those of the PC plates at 25 Hz and 100 Hz, but they decrease overall in other regions. The similar tendency shown between the experimental and simulation results validates the enhanced vibration attenuation performance of the composite sandwich structure.

For the impact force analysis, the explicit dynamics module of the ANSYS software was utilized to simulate the dynamic response of highly transient and nonlinear physical phenomena. A finite element simulation of the impact force analysis is shown in Fig. 11. A composite sandwich structure with a core nickel foam of 3 mm and a PC plate without surface patterns were modeled and simulated. The parameters of the modeled structures and surface patterns, material properties, and bonding state of the composite layers, were defined as in the previous vibration analysis. In addition, the yield strength and tangent modulus were taken into account to consider the non-linear behaviors of the materials. The yield strength and tangent modulus of polycarbonate were set as 62 MPa and 35 MPa, respectively. The yield strength and tangent modulus of nickel foam were set as 8 MPa and 2.5 MPa, respectively. Considering the round hydraulic clamp utilized during the mass drop test, the structures were modeled as round plates, and the boundary conditions were set to have fixed conditions at the edges of the structures. The impactor was modeled with parameters equal to those of the actual impactor used in the mass drop test. The modeled impactor was defined to have a weight of 2 kg and the material properties of steel. Hexahedral elements with mesh size varying between 0.001 m and 0.003 m were used in model components. The impactor was set to drop from 500 mm height with acceleration of 9.81 m/s^2. The reaction force simulation results are shown in Fig. 12.

Fig. 12(a) shows the experimental and simulation results of PC plates without surface patterns. The graph shows good agreement between the experimental and simulation results. The peak force values are almost identical, with the experiment resulting in 2.457 kN and the simulation resulting in 2.495 kN. Fig. 12(b) shows the experimental and simulation results of composite sandwich structures with a 3 mm core nickel foam. As in the case of the PC plate, the peak force values are almost identical between the experiment and the simulation, with the experiment resulting in 1.638 kN and the simulation resulting in 1.772 kN. Based on the impact force data, the impact energy values of the experiment and simulation cases are calculated using Eq. (7). The results are shown in Table 4, where the impact energy values for the experimental and simulation cases have similar values. When

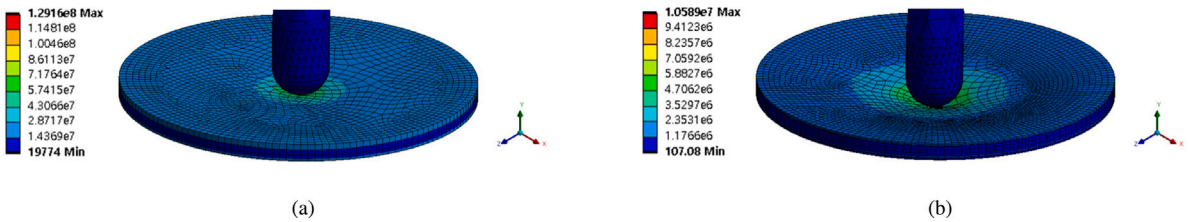

(a) (b)

Fig. 11. Finite element mass drop analysis using ANSYS. (a) Homogeneous PC plate and (b) composite sandwich plate with nickel foam core.

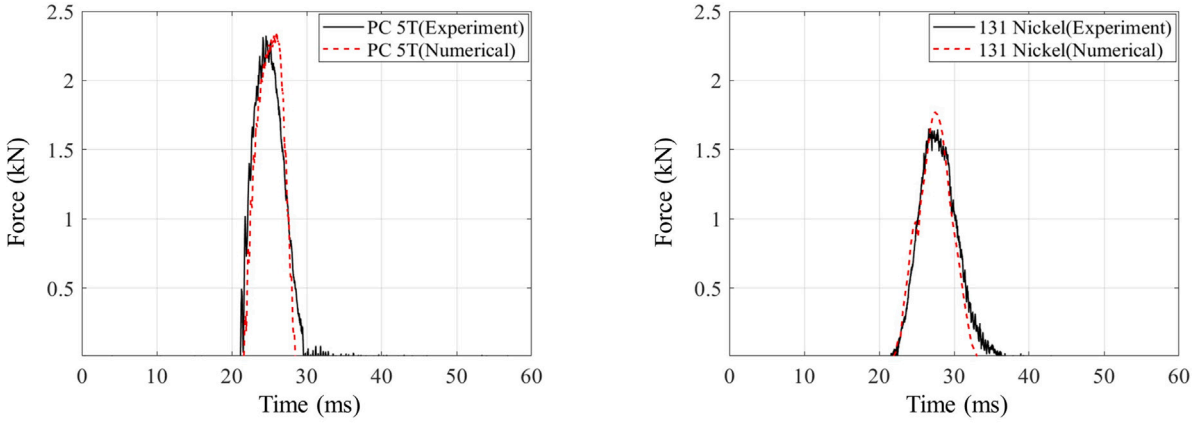

(a) (b)

Fig. 12. Shock absorption simulation results. (a) PC specimens and (b) composite specimens with nickel core thickness values of 3 mm.

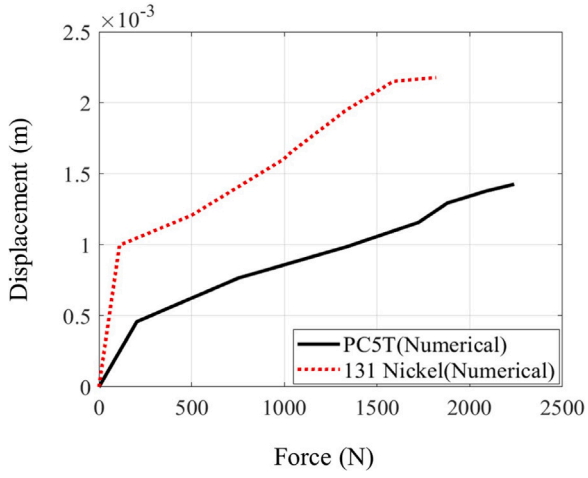

Fig. 13. The force–displacement relations of the simulated specimens.

applied with similar impact energy values, the composite specimens result in lower peak impact force values due to the increased collision time and greater specimen deformation, thus resulting in greater shock absorption. The force–displacement relations of the specimens shown in Fig. 13 supports the increased deformation of composite specimens when exposed to identical impact energy. The agreement between the experimental and the simulation results validates the experimental results in which the proposed composite sandwich structure has enhanced shock absorption performance.

The FEM-based simulation results showed trends similar to the experimental results of the vibration and impact force analyses, validating the experimental results of the impact hammer and mass drop tests. Through the FEM-based simulation, it was verified that the presence of surface patterns increases vibration attenuation, and that the presence of porous foam increases both vibration attenuation and shock absorption. Thus, the results support the utilization of porous foams and surface patterns to enhance the vibration attenuation and shock absorption in composite sandwich structures.

5. Conclusions

A composite sandwich structure with porous foam materials and surface patterns is presented in this study to achieve structural stability and mass reduction thereof. Achieving structural stability through vibration attenuation and shock absorption is a critical engineering issue. To address this issue, porous foam materials and surface patterns were utilized to increase the vibration attenuation and shock absorption performance, while achieving mass reduction. Composite sandwich structures were modeled using polycarbonate plates and porous foam materials. Copper, nickel, and PP foams were considered in the modeling of the composite structures. Laser cutting technology was used to carve the surface patterns on the top layers. Experimental studies considering impact hammer tests and mass drop tests were conducted to analyze the vibration attenuation and shock absorption performance of the composite structures. Various combinations of composite structures were considered by changing the foam materials, modifying the layer thicknesses, and considering the surface patterns. Analyses were performed to realize that the best configuration of the composite structure is the structure with core nickel foam layer of 3 mm and surface patterns on the top layer. This structure showed the greatest vibration attenuation and shock absorption performance, while simultaneously achieving mass reduction. FEM-based simulations using COMSOL and ANSYS workbench were conducted to validate the vibration attenuation and shock absorption performances of the proposed composite sandwich structure. In conclusion, this study proposes and validates the composite structural design with porous foams and surface patterns to achieve structural stability and mass reduction.

Table 4
Impact energy comparison of experiment and numerical results.

Specimen		Top layer thickness (mm)	Foam material	Foam thickness (mm)	Bottom layer thickness (mm)	Peak force (kN)	Average force (kN)	Time (ms)	Impact energy (J)
1	Experiment	5	–	–	–	2457	768.0981	8.15	9.5467
1	Numerical	5	–	–	–	2595	920.5882	6.85	9.5881
4	Experiment	1	Nickel	3	1	1638	421.2651	14.86	9.3406
4	Numerical	1	Nickel	3	1	1772	541.5224	11.56	9.4420

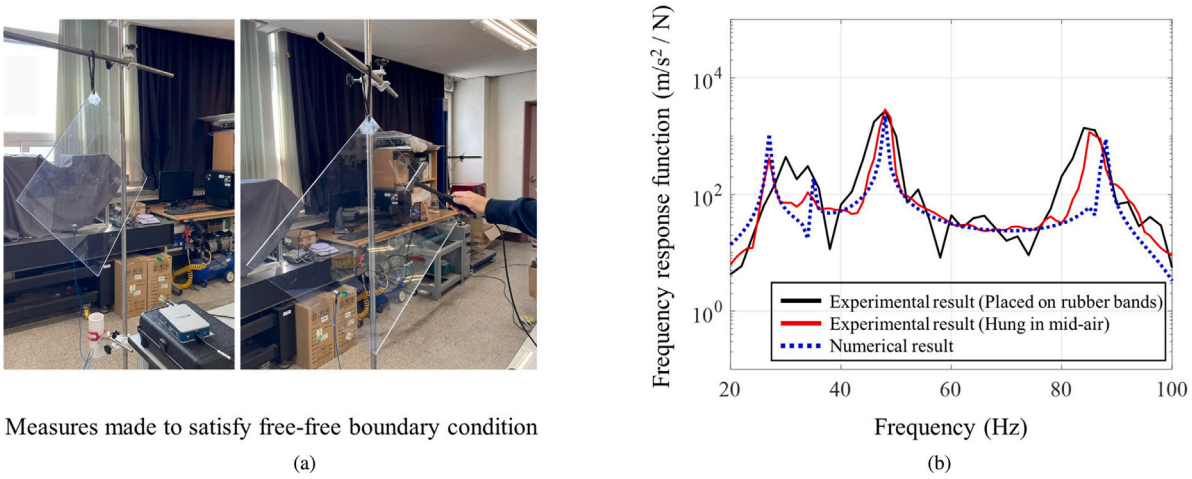

Fig. 14. Impact hammer test on PC specimen without surface patterns: (a) Hanging the specimen using rubber bands attached to the edge for achievement of free-free boundary condition and (b) comparison between results of simulation and experiments.

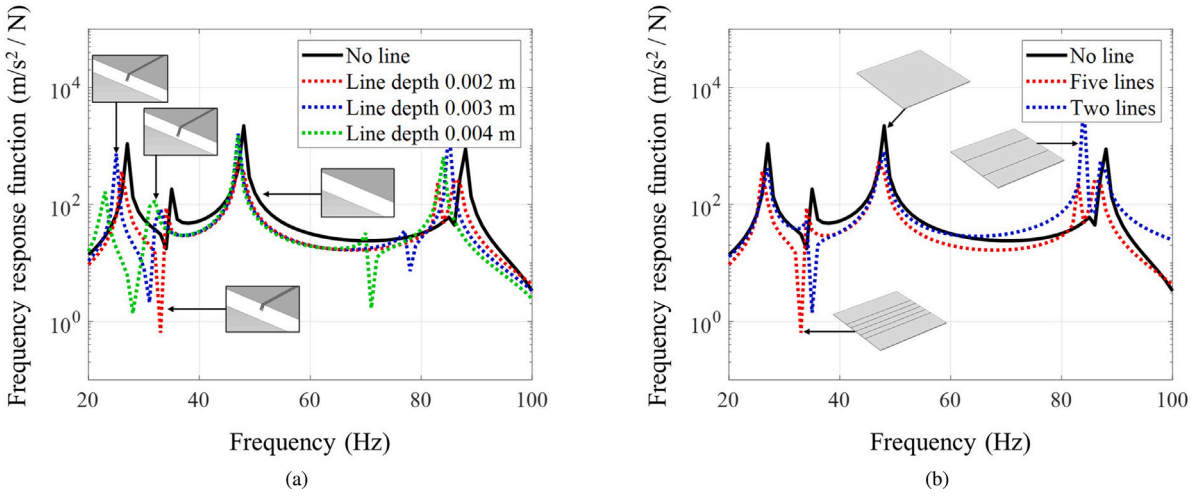

Fig. 15. Simulation results of PC plates with varying pattern parameters: (a) Decrease in natural frequency values with increasing pattern depth and (b) pattern quantity.

CRediT authorship contribution statement

Hoo Min Lee: Formal analysis, Investigation, Writing – original draft, Visualization. **Do Hyeong Kim:** Formal analysis, Investigation, Writing – original draft, Visualization. **Dong-Yoon Kim:** Formal analysis, Investigation, Writing – original draft, Visualization. **Min Seong Kim:** Formal analysis, Investigation. **Junhong Park:** Conceptualization, Validation, Resources. **Gil Ho Yoon:** Conceptualization, Methodology, Validation, Resources, Writing – review & editing, Supervision, Project administration.

Declaration of competing interest

The authors declare that they have no known competing financial interests or personal relationships that could have appeared to influence the work reported in this paper.

Acknowledgments

This work was supported by the National Research Foundation of Korea (NRF) grant funded by the Korean government (MSIT) (No. 2018R1A5A7025522) and the Police-Lab 2.0 Program (www.kipot.or.kr) grant funded by the Korean government (MSIT) and Korean National Police Agency (KNPA) (No. 082021D47000000).

Appendix A. Impact hammer test: Consideration of free-free boundary condition

Figure for the additional impact hammer test conducted to consider free-free boundary condition. (Fig. 14)

Appendix B. Pattern parameters affecting vibration attenuation performance

Figure for the effects of changing pattern parameters on vibration attenuation performance of PC plates. (Fig. 15)

References

[1] Francesconi A, Pavarin D, Bettella A, Giacomuzzo C, Faraud M, Destefanis R, et al. Generation of transient vibrations on aluminum honeycomb sandwich panels subjected to hypervelocity impacts. Int J Impact Eng 2008;35(12):1503–9.

[2] Vaidya UK, Pillay S, Bartus S, Ulven CA, Grow DT, Mathew B. Impact and post-impact vibration response of protective metal foam composite sandwich plates. Mater Sci Eng A 2006;428(1–2):59–66.

[3] Lu J, Wang Y, Zhai X. Response of flat steel-concrete-corrugated steel sandwich panel under drop-weight impact load by a hemi-spherical head. J Build Eng 2021;102890.

[4] Zhang C, Tan K. Low-velocity impact response and compression after impact behavior of tubular composite sandwich structures. Composites B 2020;193:108026.

[5] Yang B, Wang Z, Zhou L, Zhang J, Tong L, Liang W. Study on the low-velocity impact response and CAI behavior of foam-filled sandwich panels with hybrid facesheet. Compos Struct 2015;132:1129–40.

[6] Mines R, Worrall C, Gibson A. The static and impact behaviour of polymer composite sandwich beams. Composites 1994;25(2):95–110.

[7] Nan L, Tahar MB, Liang M, Fusheng S. Reduction of vibration by periodically stitched sandwich panel. Chin J Aeronaut 2021;34(7):39–49.

[8] Park S, Beak J, Kim K, Park Y-J. Study on reduction effect of vibration propagation due to internal explosion using composite materials. Int J Concr Struct Mater 2021;15(1):1–20.

[9] Chen J, Sun C. Reducing vibration of sandwich structures using antiresonance frequencies. Compos Struct 2012;94(9):2819–26.

[10] Meng H, Huang X, Chen Y, Theodossiades S, Chronopoulos D. Structural vibration absorption in multilayered sandwich structures using negative stiffness nonlinear oscillators. Appl Acoust 2021;182:108240.

[11] Shen M, Nagamura K, Nakagawa N, Okamura M. Noise reduction through elastically restrained sandwich polycarbonate window pane into rectangular cavity. J Vib Control 2013;19(3):415–28.

[12] Shen M, Nagamura K, Nakagawa N, Okamura M. Improvement noise insulation performance of polycarbonate pane using sandwich structure. J Syst Des Dyn 2012;6(1):61–72.

[13] Qi J, Li C, Tie Y, Zheng Y, Duan Y. Energy absorption characteristics of origami-inspired honeycomb sandwich structures under low-velocity impact loading. Mater Des 2021;207:109837.

[14] Zhao Y, Sun Y, Li R, Sun Q, Feng J. Response of aramid honeycomb sandwich panels subjected to intense impulse loading by Mylar flyer. Int J Impact Eng 2017;104:75–84.

[15] Torre L, Kenny J. Impact testing and simulation of composite sandwich structures for civil transportation. Compos Struct 2000;50(3):257–67.

[16] Heimbs S, Cichosz J, Klaus M, Kilchert S, Johnson A. Sandwich structures with textile-reinforced composite foldcores under impact loads. Compos Struct 2010;92(6):1485–97.

[17] Fan J, Njuguna J. An introduction to lightweight composite materials and their use in transport structures. In: Lightweight composite structures in transport. Elsevier; 2016, p. 3–34.

[18] Kim PC, et al. Composite sandwich constructions for absorbing the electromagnetic waves. Compos Struct 2009;87(2):161–7.

[19] Lopatnikov SL, Gama BA, Haque MJ, Krauthauser C, Gillespie Jr. JW, Guden M, et al. Dynamics of metal foam deformation during Taylor cylinder–Hopkinson bar impact experiment. Compos Struct 2003;61(1–2):61–71.

[20] Rakow JF, Waas AM. Response of actively cooled metal foam sandwich panels exposed to thermal loading. AIAA J 2007;45(2):329–36.

[21] Rakow JF, Waas AM. Size effects in metal foam cores for sandwich structures. AIAA J 2004;42(7):1331–7.

[22] Ebrahimi F, Seyfi A. Studying propagation of wave of metal foam rectangular plates with graded porosities resting on Kerr substrate in thermal environment via analytical method. Waves Random Complex Media 2020;1–24.

[23] Magnucka-Blandzi E, Magnucki K. Effective design of a sandwich beam with a metal foam core. Thin-Walled Struct 2007;45(4):432–8.

[24] Bledzki AK, Kirschling H, Steinbichler G, Egger P. Polycarbonate microfoams with a smooth surface and higher notched impact strength. J Cellular Plast 2004;40(6):489–96.

[25] Bledzki AK, Rohleder M, Kirschling H, Chate A. Correlation between morphology and notched impact strength of microcellular foamed polycarbonate. J Cellular Plast 2010;46(5):415–40.

[26] Srivastava V. Impact behaviour of sandwich GFRP-foam-GFRP composites. Int J Compos Mater 2012;2(4):63–6.

[27] Sierakowski R, Hughes M. Force protection using composite sandwich structures. Compos Sci Technol 2006;66(14):2500–5.

[28] Vo NH, Pham TM, Bi K, Chen W, Hao H. Stress wave mitigation properties of dual-meta panels against blast loads. Int J Impact Eng 2021;154:103877.

[29] Zhou Q, Yin X, Ye F, Mo R, Tang Z, Fan X, et al. Optically transparent and flexible broadband microwave metamaterial absorber with sandwich structure. Appl Phys A 2019;125(2):131.

[30] He L, Shan D, He J, Liu S, Chen Z, Xu H. Low-frequency perfect sandwich meta-absorber based on magnetic metal. Modern Phys Lett B 2019;33(06):1950057.

[31] Liu J, Liu J, Mei J, Huang W. Investigation on manufacturing and mechanical behavior of all-composite sandwich structure with Y-shaped cores. Compos Sci Technol 2018;159:87–102.

[32] Mei J, Liu J, Huang W. Three-point bending behaviors of the foam-filled CFRP X-core sandwich panel: experimental investigation and analytical modelling. Compos Struct 2022;115206.

[33] Zhao Y, Yang Z, Yu T, Xin D. Mechanical properties and energy absorption capabilities of aluminium foam sandwich structure subjected to low-velocity impact. Constr Build Mater 2021;273:121996.

[34] Sharei A, Safarabadi M, Mashhadi MM, Solut RS, Haghighi-Yazdi M. Experimental and numerical investigation of low velocity impact on hybrid short-fiber reinforced foam core sandwich panel. J Compos Mater 2021;55(29):4375–85.

[35] Warnet L, Reed P. Falling weight impact testing principles. In: Mechanical properties and testing of polymers. Springer; 1999, p. 66–70.